Mental Disease 191, 503-508.

Ramanaiah, N.V., Rielage, J.K., Cheng, Y., 2002. Cloninger's temperament and character inventory and the NEO Five-Factor Inventory. Psychological Reports 90, 1059-1063.

Sheehan, D.V., Lecrubier, Y., Sheehan, K.H., Amorim, P., Janavs, J., Weiller, E., Hergueta, T., Baker, R., Dunbar, G.C., 1998. The Mini-International Neuropsychiatric Interview (M.I.N.I.): the development and validation of a structured diagnostic psychiatric interview for DSM-IV and ICD-10. Journal of Clinical Psychiatry 59 (suppl. 20), 22-57.

Svrakic, D.M., Draganic, S., Hill, K., Bayon, C., Przybeck, T.R., Cloninger, C.R., 2002. Temperament, character, and personality disorders: etiologic, diagnostic, treatment issues. Acta Psychiatrica Scandinavica 106, 189-195.

Svrakic, D.M., Whitehead, C., Przybeck, T.R., Cloninger, C.R., 1993. Differential diagnosis of personality disorders by the seven-factor model of temperament and character. Archives of General Psychiatry 50, 991-999.

Toomey, R., Kremen, W.S., Simpson, J.C., Samson, J.A., Seidman, L.J., Lyons, M.J., Faraone, S.V., Tsuang, M.T., 1997. Revisiting the factor structure for positive and negative symptoms: evidence from a large heterogeneous group of psychiatric patients. American Journal of Psychiatry 154, 371-377.

Van Os, J., Jones, P.B., 2001. Neuroticism as a risk factor for schizophrenia. Psychological Medicine 31, 1129-1134.

Figure legends

Fig. 1. Mean scores on 7 dimensions of TCI in schizophrenia males.

■, schizophrenia males; □, schizophrenia females; □, total controls (male and female combined). *Only schizophrenia males significantly differed from controls; **Both schizophrenia males and females significantly differed from controls.

Table 1

Demographic and clinical characteristics of patients with schizophrenia and healthy controls stratified by gender

Characteristic	Schizophrenia patients (n = 86)		Analyses (male vs. female patients)		Healthy controls (n = 115)		Analyses (male vs. female controls)	
	Male (n = 53)	Female (n = 33)	statistics	P	Male (n = 71)	Female (n = 44)	statistics	P
Age, years: mean (S.D.)	41.5 (11.8)	41.9 (10.6)	$F(1,84) = 0.025$	0.87	41.2 (14.0)	41.6 (4.1)	$F(1,113) = 0.046$	0.83
Education, years: mean (S.D.)	13.6 (2.6)	13.1 (1.7)	$F(1,84) = 1.19$	0.28	17.3 (3.0)	14.4 (1.9)	$F(1,113) = 31.9$	< 0.001
Family history of psychiatric disease: Yes/No	20/33	9/24	$\chi2(1) = 0.996$	0.32				
Age at illness onset, years: mean (S.D.)	23.6 (6.6)	25.1 (8.8)	$F(1,84) = 0.83$	0.36				
Duration of illness, years: mean (S.D.)	17.9 (11.4)	16.8 (10.1)	$F(1,84) = 0.22$	0.64				
CPZeq of total antipsychotics, mg/day: mean (S.D.)	974.5 (927.5)	837.6 (690.8)	$F(1,84) = 0.53$	0.47				
Number of hospitalizations, n: mean (S.D.)	2.3 (2.1)	2.2 (2.7)	$F(1,84) = 0.061$	0.81				
Outpatients/Inpatients, n	35/18	22/11	$\chi2(1) = 0.0036$	0.95				

PANSS scores (n = 53): mean (S.D.)	(n = 31)	(n = 22)		
Positive subscale	13.3 (5.6)	15.8 (7.7)	$F(1,51) = 1.79$	0.19
Negative subscale	20.5 (6.9)	18.9 (7.0)	$F(1,51) = 0.63$	0.43
General subscale	29.0 (8.8)	30.1 (8.1)	$F(1,51) = 0.20$	0.66
Total score	62.8 (16.8)	64.8 (18.9)	$F(1,51) = 0.16$	0.69

CPZeq: Chlorpromazine equivalents.

PANSS: Positive and Negative Syndrome Scale (Kay et al., 1987).

Table 2

Comparisons of TCI scores between patients with schizophrenia and control subjects

Variable		No. of items	Schizophrenia patients (n = 86) Mean (S.D.)	Healthy controls (n = 115) Mean (S.D.)	ANOVA [a]		ANCOVA [b]	
					F	P	F	P
Novelty seeking	NS	40	17.4 (4.6)	20.6 (4.1)	26.69	< 0.001	27.79	< 0.001
Harm avoidance	HA	35	22.7 (6.0)	16.9 (5.6)	48.4	< 0.001	40.87	< 0.001
Reward dependence	RD	24	13.6 (3.5)	15.2 (3.7)	9.86	0.002	13.55	< 0.001

Persistence	PS	8	4.1 (1.9)	4.6 (1.7)	3.81	0.052	0.36	0.55
Self-directedness	SD	44	23.6 (6.6)	30.1 (5.8)	55.07	< 0.001	32.64	< 0.001
Cooperativeness	CO	42	26.7 (5.4)	28.5 (5.4)	5.38	0.02	5.18	0.02
Self-transcendence	ST	33	13.8 (7.5)	10.9 (5.1)	10.79	0.001	5.24	0.02

[a] Degrees of freedom = 1, 199.

[b] Education years was controlled for. Degrees of freedom = 1, 199.

Table 3

Correlations between TCI and PANSS scores

	NS	HA	RD	PS	SD	CO	ST
Positive subscale	0.02	-0.14	-0.10	0.23	-0.17	-0.04	0.34*
Negative subscale	0.04	0.11	-0.34*	-0.27*	-0.25	-0.28*	-0.25
General subscale	0.26	0.004	-0.37**	0.03	-0.32*	-0.29*	0.16
Total score	0.15	-0.01	-0.35**	-0.01	-0.32*	-0.27	0.11

Each figure represents Pearson's *r*.

* $P < 0.05$, ** $P < 0.01$.

Table 4

Comparisons of TCI results in schizophrenia patients and healthy controls between prior studies and ours

	Country (City)	No. of sample		Matching	TCI results (patients vs. controls)[a]						
		Patients	Controls	status	NS	HA	RD	PS	SD	CO	ST
The present study	Japan (Tokyo)	86	115	age/gender	-3.2**	5.8**	-1.6**	-0.5	-6.5**	-1.8*	2.9**
Guillem et al. (2002)	Canada (Montreal)	52	25	age	-4.4**	8.1**	-0.9	-1.4*	-8.1**	-3.6**	2.4
Boeker et al. (2006)	Germany (Magdeburg)	22	22	age/gender	-0.4	2.9	0.4	-0.4	-5.9**	-2.8*	4.1*

[a] Differences in sub-dimensions of TCI between patients and controls of each study.

Each figure in these 7 columns was calculated as follows: <mean of patients> - <mean of controls>

*: Patients showed a significant difference from controls ($P < 0.05$).

**: Patients showed a significant difference from controls ($P < 0.01$).

Fig. 1.

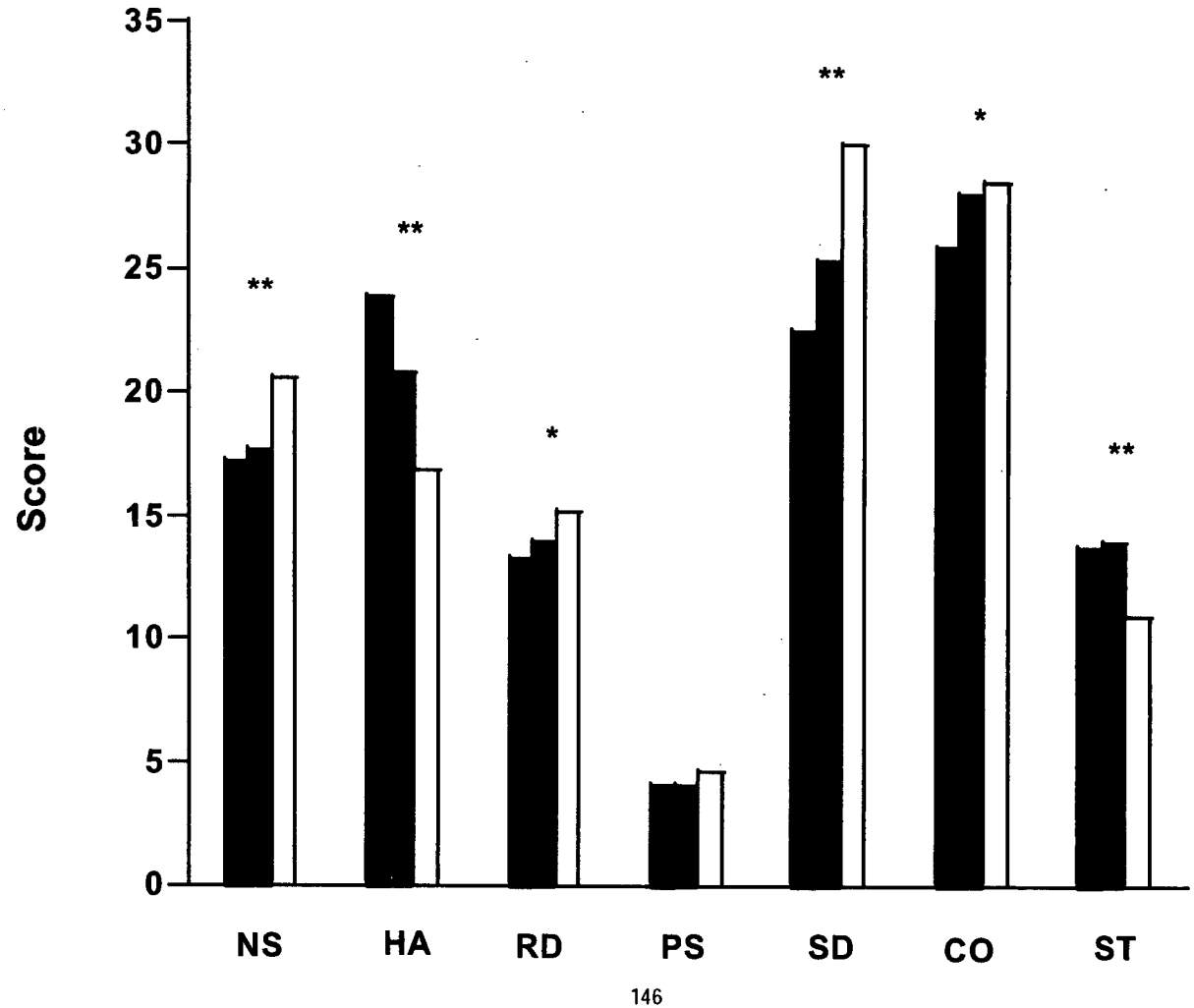

SCHRES-03383; No of Pages 3

Available online at www.sciencedirect.com

ScienceDirect

Schizophrenia Research xx (2007) xxx – xxx

SCHIZOPHRENIA RESEARCH

www.elsevier.com/locate/schres

Letter to the Editors

No association between the NDE1 gene and schizophrenia in the Japanese population

Dear Editors,

Series of studies have implicated that Disrupted in Schizophrenia 1 (DISC1) and its pathways are in the pathophysiology of schizophrenia (SZ) (Callicott et al., 2005; Hennah et al., 2003; Yamada et al., 2004). Recently, Hennah et al reported that the schizophrenic samples for the presence of SZ risk allelic haplotype (HEP3) of the DISC1 gene displayed an evidence for linkage of 16p13 (LOD=3.17) that contains the NDE1 gene. In addition, they also showed a significant association between specific haplotypes of the NDE1 gene (rs4781678-rs2242549-rs881803-rs2075512) and affected females with SZ spectrum disorders (Hennah et al., 2007). The NDE1 gene encodes a protein which interacts with the DISC1 protein (Millar et al., 2003; Brandon et al., 2004) and mouse models with NDE1 homozygous mutations displayed disordered cortex (Feng and Walsh, 2004). To confirm the association of the NDE1 gene with SZ, we performed the case-control association study in the Japanese population.

We used genomic DNA samples from 726 SZ patients: 406 male (mean age: 48.6±13.8 years), 320 female (mean age: 49.2±14.5 years) from the Tokushima University Hospital, affiliated psychiatric hospitals of the University of Tokushima, the Ehime University Hospital and the Osaka University Hospital in Japan. The diagnosis of SZ was made by at least two experienced psychiatrists according to DSM-IV criteria. 744 controls: 419 male (mean age: 45.8±11.3 years), 325 female (mean age: 45.2± 10.5) were selected from volunteers without the psychiatric problems. All subjects were unrelated Japanese origin and signed written informed consent to participate in the genetic association studies approved by the institutional ethics committees. Genotyping was performed using commercially available TaqMan probes for the NDE1 gene with the Applied Biosystems 7500 Fast Real Time PCR System. We selected seven single nucleotide polymorphic (SNP) markers for genotyping from the public databases (dbSNP Home page) as reference for International Hap Map Project and Hennah's report (Hennah et al., 2007). The SNPs we selected includes six of seven of Hennah's because they are suitable for association study in the Japanese population. Haplotype block structure was determined using the HAPLOVIEW program (Barrett et al., 2005) defined according to the criteria of Gabriel et al. (Gabriel et al., 2002). Allelic and genotypic frequencies of patients and control subjects were compared using Fisher's exact test. The SNPAlyze 3.2Pro software (DYNACOM, Japan) was used to estimate haplotype frequencies, LD, permutation p values (10,000 replications) and deviation from Hardy–Weinberg (HW) distribution of alleles. Pair-wise LD indices (D' and r^2) were calculated for the control subjects. Power calculations for our sample size performed using the G*Power program (Erdfelder et al., 1996). The criterion for significance was set at $p<0.05$ for all tests.

Genotypic and allelic frequencies of the NDE1 gene are shown in Table 1. In power calculations using the G*Power program, our sample size had >0.97 power for detecting a significant association (alpha<0.05) when an effect size index of 0.2 was used. Genotypic distributions of these seven SNPs did not deviate significantly from HW equilibrium in either group ($p>0.05$). There were no significant differences in genotypic and allelic frequencies between cases and controls in all seven SNPs. LD between each pair of all the SNPs is relatively high ($D'\geqq 0.76$, $r^2\geqq 0.39$). There were two LD blocks in NDE1 with rs2242549 and rs881803 residing in block 1 and rs2075512 and rs2384933 residing in block 2. The two marker haplotypes of block 1 and block 2 were not associated with SZ (permutation $p=0.93$, 0.36, respectively). When the data were subdivided on the basis of gender, no significant association was observed in seven SNPs either in male or female samples. The two marker haplotypes of block 1 and block 2 were not associated with SZ either in male and female (permutation p of block 1=0.73 and 0.26, permutation p of block 2=0.49 and 0.21, respectively). In addition, a tag-haplotype (rs4781678-rs2242549-rs881803-rs2075512) that Hennah et al reported a significant association with SZ

0920-9964/$ - see front matter © 2007 Published by Elsevier B.V.
doi:10.1016/j.schres.2007.10.032

Please cite this article as: Numata, S., et al., No association between the NDE1 gene and schizophrenia in the Japanese population, Schizophr. Res. (2007), doi:10.1016/j.schres.2007.10.032

t1.1 Table 1
t1.2 Genotypes and allele frequencies for the seven polymorphism

t1.3 SNP	Total samples									Female			Male		
t1.4	Diagnosis	Allele		p-value genotype				p-value frequency		Allele		p-value	Allele		p-value
t1.5		C	A		C/C	C/A	A/A			C	A		C	A	
t1.6 rs4781678	SZ	923	519	0.56	299	325	97	0.75	0.36	408	226	0.91	515	293	0.54
t1.7	CT	963	517		321	321	98		0.349	420	228		543	289	
t1.8		C	T		C/C	C/T	T/T			C	T		C	T	
t1.9 rs6498567	SZ	814	632	0.5	226	362	135	0.58	0.437	347	289	0.26	467	343	0.96
t1.10	CT	851	627		249	353	137		0.424	372	272		479	355	
t1.11		T	G		T/T	T/G	G/G			T	G		T	G	
t1.12 rs2242549	SZ	762	690	0.61	196	370	160	0.35	0.475	324	316	0.22	438	374	0.69
t1.13	CT	793	691		221	351	170		0.466	352	298		441	393	
t1.14		C	T		C/C	C/T	T/T			C	T		C	T	
t1.15 rs881803	SZ	689	761	0.66	159	371	195	0.47	0.475	320	318	0.13	369	443	0.49
t1.16	CT	694	794		168	358	218		0.466	298	352		396	442	
t1.17		C	T		C/C	C/T	T/T			C	T		C	T	
t1.18 rs2075512	SZ	714	736	0.51	174	366	185	0.51	0.492	316	324	0.87	398	412	0.49
t1.19	CT	751	737		197	357	190		0.505	324	326		427	411	
t1.20		C	T		C/C	C/T	T/T			C	T		C	T	
t1.21 rs2384933	SZ	936	516	0.54	298	340	88	0.71	0.355	414	226	0.68	522	290	0.64
t1.22	CT	976	512		321	334	89		0.344	428	222		548	290	
t1.23		G	A		G/G	G/A	A/A			G	A		G	A	
t1.24 rs11130	SZ	699	741	0.55	162	375	183	0.07	0.485	313	323	1	386	418	0.43
t1.25	CT	738	748		197	344	202		0.497	320	330		418	418	

spectrum disorders in female was not associated with SZ either in male and female (permutation $p=0.90$, 0.054, respectively) of the Japanese population.

Although an association between specific haplotypes of NDE1 and a broad spectrum of SZ specific females was reported (Hennah et al., 2007), we could not replicate significant associations between seven NDE1 SNPs and SZ in our Japanese samples. Different results between our study and Hennah's study may be that (a) different end-state diagnosis subjects used; Hennah et al used a broad spectrum of SZ including SZ, schizoaffective disorder, schizophrenia spectrum conditions and mood disorder, (b) ethnic difference; different allele frequency and different LD patterns (Supplementary Table), (c) different sample size.

In conclusion, we failed to find the association between the NDE1 gene and SZ in the Japanese population. This gene may not play a major role in the etiology of SZ. However we can not rule out a possibility that DISC1-NDE1 interaction may be involved in the etiology of schizophrenia. Further studies will be needed to conclude whether DISC1-NDE1 interaction is associated with SZ.

Acknowledgement

This work was supported by a Grant-in-Aid for Scientific Research from the Japanese Ministry of Education, Culture, Sports, Science and Technology and a Grant-in-Aid for Scientific Research from the 21st Century COE program, Human Nutritional Science on Stress Control, Tokushima, Japan.

Appendix A. Supplementary data

Supplementary data associated with this article can be found, in the online version, at doi:10.1016/j.schres.2007.10.032.

References

Barrett, J.C., Fey, B., Maller, J., Daly, M.J., 2005. Haplowiew: analysis and visualization of LD and haplotype maps. Bioinformatics 21, 263–265.

Brandon, N.J., Handford, E.J., Schurov, I., Rain, J.C., Pelling, M., Duran-Jimeniz, B., Camargo, L.M., Oliver, K.R., Beher, D., Shearman, M.S., Whiting, P.J., 2004. Disrupted in schizophrenia 1 and Nudel form a neurodevelopmentally regulated protein complex: implications for schizophrenia and other major neurological disorders. Mol. Cell. Neurosci. 25, 42–55.

Callicott, J.H., Straub, R.E., Pezawas, L., Egan, M.F., Mattay, V.S., Hariri, A.R., Verchinski, B.A., Meyer-Lindenberg, A., Balkissoon, R., Kolachana, B., Goldberg, T.E., Weinberger, D.R., 2005. Variation in DISC1 affects hippocampal structure and function and increases risk for schizophrenia. Proc. Natl. Acad. Sci. U.S.A. 102, 8627–8632.

Erdfelder, E., Faul, F., Buchner, A., 1996. GPOWER: a general power analysis program. Behav. Res. Meth. Instrum. Comput. 28, 1–11.

Feng, Y., Walsh, C.A., 2004. Mitotic spindle regulation by Nde1 controls cerebral cortical size. Neuron 44, 279–293.

Gabriel, S.B., Schaffner, S.F., Nguyen, H., Moore, J.M., Roy, J., Blumenstiel, B., Higgins, J., DeFelice, M., Lochner, A., Faggart, M., Liu-Cordero, S.N., Rotimi, C., Adeyemo, A., Cooper, R., Ward, R., Lander, E.S., Daly, M.J., Altshuler, D., 2002. The structure of haplotype blocks in the human genome. Science 296, 2225–2229.

Hennah, W., Varilo, T., Kestila, M., Paunio, T., Arajarvi, R., Haukka, J., Parker, A., Martin, R., Levitzky, S., Partonen, T., Meyer, J., Lonnqvist, J., Peltonen, L., Ekelund, J., 2003. Haplotype transmission analysis provides evidence of association for DISC1 to schizophrenia and suggests sex-dependent effects. Hum. Mol. Genet. 12, 3151–3159.

Hennah, W., Tomppo, L., Hiekkalinna, T., Palo, O.M., Kilpinen, H., Ekelund, J., Tuulio-Henriksson, A., Silander, K., Partonen, T., Paunio, T., Terwilliger, J.D., Lonnqvist, J., Peltonen, L., 2007. Families with the risk allele of DISC1 reveal a link between schizophrenia and another component of the same molecular pathway, NDE1. Hum. Mol. Genet. 16, 453–462.

Millar, J.K., Christie, S., Porteous, D.J., 2003. Yeast two-hybrid screens implicate DISC1 in brain development and function. Biochem. Biophys. Res. Commun. 311, 1019–1025.

Yamada, K., Nakamura, K., Minabe, Y., Iwayama-Shigeno, Y., Takao, H., Toyota, T., Hattori, E., Takei, N., Sekine, Y., Suzuki, K., Iwata, Y., Miyoshi, K., Honda, A., Baba, K., Katayama, T., Tohyama, M., Mori, N., Yoshikawa, T., 2004. Association analysis of FEZ1 variants with schizophrenia in Japanese cohorts. Biol. Psychiatry 56, 683–690.

Shusuke Numata
Shu-ichi Ueno*
Jun-ichi Iga
Masahito Nakataki
Tetsuro Ohmori
Department of Psychiatry,
Course of Integrated Brain Sciences,
Medical Informatics, Institute of Health Biosciences,
The University of Tokushima Graduate School, Japan
*Corresponding author. Department of Community and Psychiatric Nursing, School of Health Sciences, The University of Tokushima Graduate School, 18-15 Kuramoto-cho 3, Tokushima 770-8509, Japan. Tel./fax: +81 88 633 9023.
E-mail address: shuichi@medsci.tokushima-u.ac.jp (S.Ueno).

Shu-ichi Ueno
Department of Community and Psychiatric Nursing,
Major in Nursing, School of Health Sciences,
The University of Tokushima Graduate School, Japan

Toshihito Tanahashi
Mitsuo Itakura
Division of Genetic Information,
Institute for Genome Research,
The University of Tokushima Graduate School, Japan

Akira Sano
Department of Psychiatry, Kagoshima University
Graduate School of Medical and Dental Science, Japan

Ryota Hashimoto
Masatoshi Takeda
The Osaka-Hamamatsu Joint Research Center
For Child Mental Development,
Osaka University Graduate school of Medicine, Japan

Kazutaka Ohi
Ryota Hashimoto
Masatoshi Takeda
Department of Psychiatry,
Osaka University Graduate school of Medicine, Japan

23 August 2007

Please cite this article as: Numata, S., et al., No association between the NDE1 gene and schizophrenia in the Japanese population, Schizophr. Res. (2007), doi:10.1016/j.schres.2007.10.032

J Hum Genet
DOI 10.1007/s10038-008-0251-9

ORIGINAL ARTICLE

Dynamin 2 gene is a novel susceptibility gene for late-onset Alzheimer disease in non-*APOE*-ε4 carriers

Nuripa Jenishbekovna Aidaralieva · Kouzin Kamino · Ryo Kimura · Mitsuko Yamamoto · Takeshi Morihara · Hiroaki Kazui · Ryota Hashimoto · Toshihisa Tanaka · Takashi Kudo · Tomoyuki Kida · Jun-Ichiro Okuda · Takeshi Uema · Hidehisa Yamagata · Tetsuro Miki · Hiroyasu Akatsu · Kenji Kosaka · Masatoshi Takeda

Received: 6 November 2007 / Accepted: 30 December 2007

Abstract Alzheimer disease (AD) is characterized by progressive cognitive decline caused by synaptic dysfunction and neurodegeneration in the brain, and late-onset AD (LOAD), genetically classified as a polygenetic disease, is the major form of dementia in the elderly. It has been shown that β amyloid, deposited in the AD brain, interacts with dynamin 1 and that the dynamin 2 (*DNM2*) gene homologous to the dynamin 1 gene is encoded at chromosome 19p13.2 where a susceptibility locus has been detected by linkage analysis. To test the genetic association of LOAD with the *DNM2* gene, we performed a case–control study of 429 patients with LOAD and 438 sex- and age-matched control subjects in a Japanese population. We found a significant association of LOAD with single nucleotide polymorphism markers of the *DNM2* gene, especially in non-carriers of the apolipoprotein E-ε4 allele. Even though subjects with the genotype homozygous for the risk allele at rs892086 showed no mutation in exons of the *DNM2* gene, expression of *DNM2* mRNA in the hippocampus was decreased in the patients compared to non-demented controls. We propose that the *DNM2* gene is a novel susceptibility gene for LOAD.

Keywords Alzheimer · Apolipoprotein E · Association · Chromosome 19p · Dynamin 2 · Genetic risk

Electronic supplementary material The online version of this article (doi:10.1007/s10038-008-0251-9) contains supplementary material, which is available to authorized users.

N. J. Aidaralieva · K. Kamino (✉) · R. Kimura · M. Yamamoto · T. Morihara · H. Kazui · R. Hashimoto · T. Tanaka · T. Kudo · M. Takeda
Department of Psychiatry,
Osaka University Graduate School of Medicine,
Suita, Osaka 565-0871, Japan
e-mail: kkamino@psy.med.osaka-u.ac.jp

K. Kamino · T. Kida · J.-I. Okuda
Shoraiso National Hospital, Yamatokoriyama, Nara, Japan

T. Uema
Department of Psychiatry, Osaka General Medical Center,
Osaka, Japan

H. Yamagata
Department of Preventive Medicine,
Ehime University Graduate School of Medicine,
Toon, Ehime, Japan

T. Miki
Department of Geriatric Medicine,
Ehime University Graduate School of Medicine,
Toon, Ehime, Japan

H. Akatsu · K. Kosaka
Choju Medical Institute, Fukushimura Hospital,
Toyohashi, Aichi, Japan

Introduction

Alzheimer disease (AD) is the most common form of dementia in the elderly and is characterized by progressive cognitive decline with brain atrophy that is most marked in the temporal lobes. It is thought that β amyloid is a causative molecule in AD by disturbing synaptic function, leading to neuronal death (for review, see Selkoe 2002; Yao 2004). Although both early- and late-onset AD (LOAD) exhibit the same neuropathology in the brain, LOAD is genetically classified as a polygenetic disease and is characterized by more heterogeneous conditions than autosomal dominant early-onset AD. Apolipoprotein E (*APOE*) has been shown to be a major risk factor for LOAD (Corder et al. 1993; Farrer et al. 1997). Genome scans of LOAD detected several susceptibility loci, among

which chromosomes 12, 10 and 9 have been the targets of searches for risk genes (Pericak-Vance et al. 1997; Blacker et al. 2003). Multipoint linkage analysis of LOAD families have also demonstrated a susceptibility locus at 19p13.2 between D19S391and D19S914 (Wijsman et al. 2004).

The major role of the dynamin proteins is in the endocytosis of vesicles, and its functions in vesicle budding have been described as being responsible for the constriction of the lipid neck, fission of lipids and regulation of the scission reaction (for review, see Praefcke and McMahon 2004). Expression of the dynamin 2 (*DNM2*) as well as dynamin 1 (*DNM1*) gene is downregulated by β amyloid in hippocampal neurons (Kelly et al. 2005), suggesting that the dynamin proteins are involved in the cascade of neurodegeneration caused by β amyloid. The dynamin-binding protein (*DNMBP*) gene on chromosome 10 has also been shown to be associated with LOAD (Kuwano et al. 2006). We observed that the *DNM2* gene is located at 19p13.2, within the region where a susceptibility locus was noted (Wijsman et al. 2004). Therefore, the *DNM2* gene could be a positional and functional candidate for a genetic risk for LOAD.

To examine whether the *DNM2* gene is genetically associated with LOAD, we performed an age- and sex-matched case–control study in a Japanese population. We propose herein that the *DNM2* gene is a novel genetic factor for LOAD in non-*APOE*-ε4 carriers.

Subjects and methods

Study subjects

Patients with LOAD were diagnosed as having definite or probable AD according to the criteria of the National Institute of Neurological and Communicative Disorders and Stroke–Alzheimer's Disease and Related Disorders Association (NINCDS–ADRDA) (McKhann et al. 1984). Controls consisted of non-demented elderly subjects obtained from the general population. Written informed consent to participate in this study was obtained, and then peripheral blood was drawn and subjected to DNA extraction. For a definite diagnosis of AD, dissections were carried out at the Choju Medical Institute after obtaining the agreement of the patients' guardians for diagnosis and genomic research. In total, 429 (69.9% female) patients participated in the study, of whom 66 had definite AD and 363 had probable AD. The mean age ± SD of the patient population at onset was 72.3 ± 8.1 years (range 60–94 years), and the mean age at blood drawing was 77.4 ± 8.7 years (range 60–98 years). The controls consisted of 438 individuals (63.7% female). The mean age of the controls at assessment was 74.5 ± 5.5 years (range 60–99 years). The age at onset of the patient was matched to the age of controls, and the sex composition was not different between the groups. Hippocampal tissue was also obtained from the postmortem brains of 22 patients with AD (age 82.8 ± 8.5 years, 63.6% female) and 12 controls (age 89.0 ± 7.0 years, age at onset 72.9 ± 7.2 years, 58.0% female). DNA was extracted from peripheral blood using a QIAamp DNA Blood Kit (Qiagen, Tokyo, Japan) and from brain tissue by the phenol–chloroform method (Sambrook et al. 1989). The procedure to obtain the specimens was approved by the Genome Ethical Committee of Osaka University Graduate School of Medicine, Ehime University, and the Choju Medical Institute of Fukushimura Hospital.

Genotyping and sequencing

Single nucleotide polymorphisms (SNPs) in the *DNM2* gene regions used in this study are listed in Table 1. Genotyping was performed by a quantitative genotyping method using the TaqMan SNP Genotyping System (Applied Biosystems, Foster City, CA). The genotype of the *APOE* gene was determined by a PCR-restriction fragment length polymorphism (RFLP) method (Wenham et al. 1991). DNA obtained from six patients and three controls homozygous for the risk allele at rs892086 of the *DNM2* gene was subjected to direct sequencing of its exons using the primers listed in Electronic Supplementary Material.

Quantitative real-time PCR

Total RNA was isolated from frozen hippocampal tissues using the acid guanidine–phenol–chloroform RNA extraction method provided as ISOGEN (Nippon Gene, Toyama, Japan) and purified using an RNeasy Mini kit (Qiagen, Valencia, CA). RNA samples with an A_{260}/A_{280} absorption ratio over 1.9 were subjected to cDNA synthesis using a High-Capacity cDNA Archive kit (Applied Biosystems). Primers and probe sets for the human *DNM2* and *β-actin* genes were purchased from TaqMan Gene Expression Assay products (Applied Biosystems), and quantitative real-time PCR was carried out in an ABI PRISM 7900HT (Applied Biosystems). All quantitative PCR reactions were duplicated, and the ratio of the amount of *DNM2* cDNA to that of the *β-actin* internal control cDNA was determined at the cycle threshold (CT).

Statistical analysis

Linkage disequilibrium (LD) between all pairs of biallelic loci was measured by Lewontin's D′ (|D′|) (Hedrick 1987)

Table 1 Single nucleotide polymorphism (SNP) markers in the *DNM2* gene

NCBI SNP reference ID	Location in NCBI (build 36.1)	Location	SNP sequence (allele ½)	Strand/ orientation	Minor allele
rs12974306	10691281	Intron 1	CTCTT[G/T]CCTTT	fwd/B	Allele 2
rs714307	10696405	Intron 1	CGCTA[C/T]TGCTG	fwd/B	Allele 1
rs892086	10698677	Intron 1	GTTAG[A/G]TACCA	rev/T	Allele 1
rs34626880	10701428	Intron 1	AGCTC[C/T]ACCTG	fwd/B	Allele 2
rs10775614	10728219	Intron 1	GGCAC[A/ G]TGGCG	fwd/T	Allele 2
rs7246673	10737841	Intron 2	AACCC[G/T]GCTGT	fwd/B	Allele 1
rs3826803	10744126	Intron 2	TTTCT[C/G]ATTTT	fwd/B	Allele 2
rs2043332	10752239	Intron 5	GTGAC[A/C]TCAGG	rev/T	Allele 1
rs873016	10755728	Intron 6	AAATG[A/G]TATTA	rev/T	Allele 1
rs1109376	10775829	Intron 12	AGGAT[A/G]CTTCT	fwd/T	Allele 1
rs3786719	10788100	intron 15	TGGAA[C/G]CTTCC	fwd/T	Allele 2
rs11085748	10788540	intron 15	GTTTT[C/T]CTCAT	fwd/B	Allele 2
rs3760781	10808522	3'UTR	TTGAG[C/T]GCTCA	fwd/B	Allele 2

UTR, Untranslated region; NCBI, National Center for Biotechnology Information

and r^2. Haplotype blocks, defined as segments with strong LD (Gabriel et al 2002), were calculated using HAPLOVIEW (Barrett et al. 2005). Allele and genotype frequencies were assessed for associations by one-sided chi-squared test for both allele and genotype frequencies in dominant and recessive models, where p values less than 0.05 were tentatively judged to be significant. The effective number of independent marker loci in the *DNM2* gene was calculated to correct for multiple testing, using the software SNPSPD (http://www.genepi.qimr.edu.au/general/daleN/SNPSpD/) based on the spectral decomposition of matrices of pair-wise LD between SNPs (Nyholt 2004). The experiment-wide significance threshold required to keep the type I error rate at 5% was used for judging significance to correct for multiple testing. The values obtained by quantitative PCR, having a normal distribution, were compared by Student's t test, and a p value less than 0.05 was considered to be significant.

Results

We genotyped 13 SNPs located from intron 1 to the 3′-untranslated region (UTR) of the *DNM2* gene (Table 1). In total, 429 cases and 438 sex- and age-matched controls were genotyped, and their genotype distributions of both the cases and controls were in Hardy–Weinberg equilibrium. In these datasets, the *APOE-ε4* allele was associated with LOAD ($p < 1 \times 10^{-10}$): compared to non-*APOE-ε4* carriers, the odds ratio for carrying one *APOE-ε4* allele was 4.3 [95% confidence interval (CI) 3.12–6.16] and that for carrying two *APOE-ε4* allele was 28.4 (95% CI 6.75–119). Linkage disequilibrium statistics indicated more than three haplotype blocks in the *DNM2* gene region (Fig. 1). No validated SNPs were available between rs873016 and rs1109376 at a distance of approximately 20 kb, and no strong evidence of LD was found between these two SNPs. The case–control study showed that p values of less than 0.05 were found in four SNPs located from intron 6 to the 3′UTR in terms of allele distribution, and in seven SNPs from intron 1 to the 3′UTR in terms of genotype frequencies; their odds ratios were between 1.53 and 1.75 (Table 2). Calculations with SNPSPD indicated that the effective number of independent marker loci was 8.3094 and that the experiment-wide significance threshold was 0.006. Therefore, rs3760781 remained significant after the correction for multiple testing ($p = 0.003$). To examine the interaction between the *DNM2* gene and the *APOE* gene, the cases and controls were divided into *APOE-ε4* carriers and non-*APOE-ε4* carriers. In non-*APOE-ε4* carriers, seven markers showed p values of less than 0.05, and the experiment-wide significance threshold (0.0059) supported a significant association at rs892086 ($p = 0.003$) as well as at rs3760781 ($p = 0.004$) (Table 3). However, no association was found in *APOE-ε4* carriers (data not shown), indicating that the association of the *DNM2* gene is specific for non-*APOE-ε4* carriers in our dataset.

To examine whether patients with the risk genotype could harbor any mutations in the *DNM2* gene, we sequenced all exons of the *DNM2* gene in patients and controls homozygous for the risk allele at rs892086, but we did not found any mutations, indicating that no particular mutation resulting in amino acid change is linked to the risk genotype of the *DNM2* gene. To examine the expression of the *DNM2* gene in the AD hippocampal tissue, we measured the amount of *DNM2* cDNA normalized to that of *β-actin* cDNA using quantitative PCR. Analysis of ten LOAD and eight control subjects revealed that there was significantly lower amounts of *DNM2* mRNA in the AD hippocampal tissue than in the controls ($p < 0.01$) (Fig. 2).

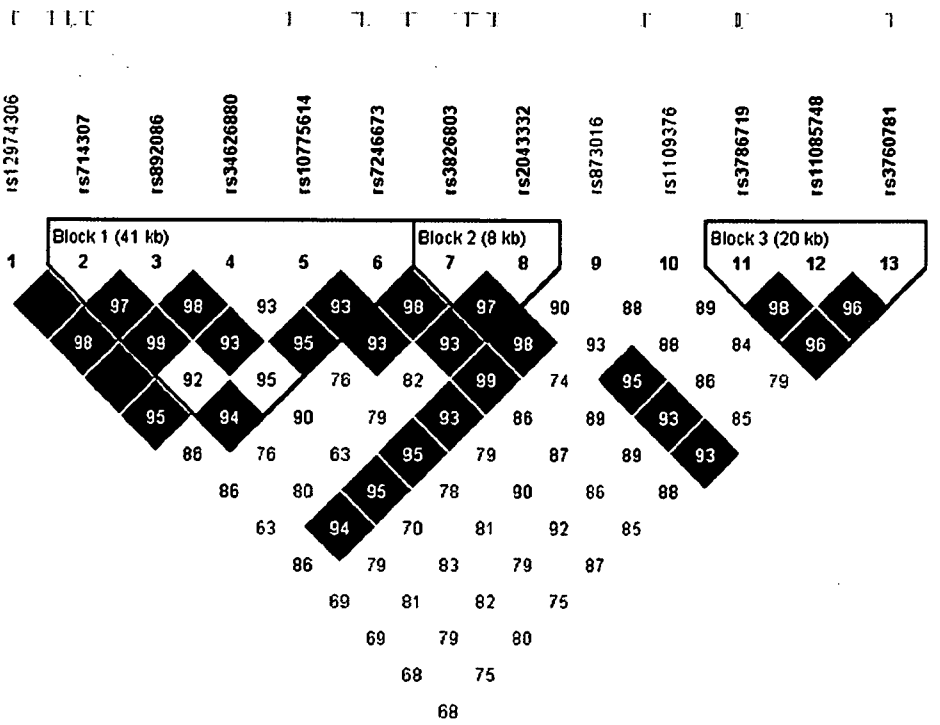

Fig. 1 Linkage disequilibrium coefficients and haplotype blocks in the *DNM2* gene region. Linkage disequilibrium coefficients (ID'I) among *DNM2* single nucleotide polymorphisms (SNPs) and haplotype blocks defined by strong LD are shown

Table 2 Association analysis of late-onset Alzheimer disease in the *DNM2* gene

SNP ID	LOAD				Control				Risk allele	*p* value	Risk genotype	*p* value	O.R (95% CI)
	Genotype number			MAF	Genotype number			MAF					
Genotype	1/1	2/2	½		1/1	2/2	½						
MArs12974306	174	57	196	0.363	204	46	188	0.320	Allele 2	NS	–	NS	
rs714307	16	285	127	0.186	16	304	117	0.170	Allele 1	NS	–	NS	
rs892086	93	134	202	0.452	67	145	226	0.411	Allele 1	NS	1/1	0.015	1.53 (1.08–2.17)
rs34626880	284	16	129	0.188	306	16	116	0.169	Allele 2	NS	–	NS	
rs10775614	306	11	111	0.155	326	14	95	0.141	Allele 2	NS	–	NS	
rs7246673	78	134	215	0.434	55	150	233	0.392	Allele 1	NS	1/1	0.020	1.56 (1.07–2.26)
rs3826803	132	86	209	0.446	145	58	234	0.400	Allele 2	NS	2/2	0.007	1.65 (1.15–2.37)
rs2043332	15	295	118	0.173	11	309	118	0.160	Allele 1	NS	–	NS	
rs873016	80	135	212	0.436	55	153	230	0.388	Allele 1	0.045	1/1	0.012	1.61 (1.11–2.33)
rs1109376	28	256	144	0.234	19	275	144	0.208	Allele 1	NS	–	NS	
rs3786719	145	85	198	0.430	166	57	215	0.376	Allele 2	0.021	2/2	0.007	1.66 (1.15–2.39)
rs11085748	138	81	209	0.433	160	56	222	0.381	Allele 2	0.027	2/2	0.013	1.59 (1.10–2.31)
rs3760781	141	87	199	0.437	157	56	225	0.385	Allele 2	0.028	2/2	0.003*	1.75 (2.21–2.52)

*Significant for experiment-wide significance threshold ($p < 0.006$)

LOAD, Late-onset Alzheimer disease; MAF, Minor Allele Frequency; O.R., odds ratio; 95% CI, 95% confidence interval

Discussion

We found that the *DNM2* gene is genetically associated with LOAD and that this association was specifically significant in non-*APOE*-ε4 carriers. In non-*APOE*-ε4 carriers, two SNPs, not in strong LD, were associated with LOAD. The *DNMBP* gene, which encodes a scaffold protein that binds to DNM1 protein, has been shown to be associated with LOAD in *APOE*-ε3*3 carriers or non-*APOE*-ε4 carriers, but not in *APOE*-ε4 carriers (Kuwano et al. 2006). Therefore, DNM2 protein could interact with proteins encoded in or linked to the *APOE*-ε3 genotype. It is

Table 3 Association analysis of late-onset Alzheimer disease in the *DNM2* gene in non-*APOE-ε4* carriers

SNP ID	LOAD				Control				Risk allele	*p* value	Risk genotype	*p* value	O.R. (95% CI)
	Genotype number			MAF	Genotype number			MAF					
	1/1	2/2	½		1/1	2/2	½						
rs12974306	87	35	97	0.381	174	37	158	0.314	Allele 2	0.019	2/2	0.033	1.71 (1.04–2.80)
rs714307	6	152	63	0.170	12	259	97	0.164	Allele 1	NS		NS	
rs892086	55	64	102	0.480	56	121	192	0.412	Allele 1	0.023	1/1	0.003*	1.85 (1.22–2.81)
rs34626880	152	6	63	0.170	260	12	97	0.164	Allele 2	NS		NS	
rs10775614	164	5	51	0.139	278	11	77	0.135	Allele 2	NS		NS	
rs7246673	41	62	117	0.452	46	127	196	0.390	Allele 1	0.037	1/1	0.041	1.61 (1.02–2.54)
rs3826803	63	42	115	0.452	121	49	198	0.402	Allele 2	NS		NS	
rs2043332	7	149	64	0.177	7	264	98	0.152	Allele 1	NS		NS	
rs873016	42	63	116	0.452	46	130	193	0.386	Allele 1	0.025	1/1	0.031	1.65 (1.04–2.60)
rs1109376	13	138	69	0.216	15	234	120	0.203	Allele 1	NS		NS	
rs3786719	71	45	104	0.441	141	47	181	0.373	Allele 2	0.021	2/2	0.013	1.76 (1.13–2.76)
rs11085748	68	44	109	0.446	136	46	187	0.378	Allele 2	0.022	2/2	0.015	1.75 (1.11–2.74)
rs3760781	73	47	100	0.441	135	46	188	0.379	Allele 2	0.037	2/2	0.004*	1.91 (1.22–2.98)

*Significant for experiment-wide significance threshold ($p < 0.0059$)

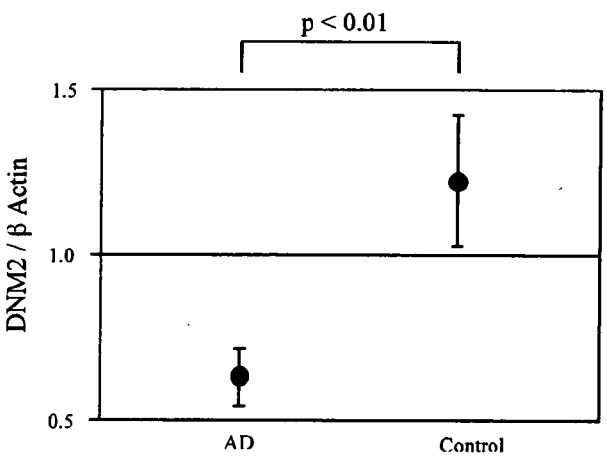

Fig. 2 Expression of *DNM2* mRNA in the hippocampus. The ratio of the amount of *DNM2* cDNA to that of *β-actin* cDNA is shown. *Dots* indicate mean value, *bars* indicate standard error

possible that the causative mechanism of DNM2 for the development of AD could be different from the lipid transfer proteins involved in lipid metabolism, such as the *APOE* (Strittmatter et al. 1993), *LRP* (Kang et al. 1997) and *CYP46* genes encoding cholesterol 24S-hydroxylase (Kolsch et al. 2002). However, the majority of cases genotyped in our study are still living, and the use of still living controls also warrants caution as the incidence of developing dementia increases with age. Therefore, our results could be misrepresented, as the controls may still develop AD, or we may have misdiagnosed AD patients who may actually have another form of dementia.

The *DNM* gene was first identified as the locus for a paralytic phenotype in *Drosophila melanogaster* (Suzuki et al. 1971) and encodes large GTPases that can associate with microtubules in vitro (Shpetner and Vallee 1989; Obar et al. 1990). The dynamin proteins are distinguished from other GTPases by their low GTP-binding affinities and the ability of many members of the dynamin family to interact with lipid membranes (for review, see Praefcke and McMahon 2004). Mutations of the pleckstrin homology domain of the *DNM2* gene, leading to diminished binding of the DNM2 protein to membranes, are responsible for Charcot–Marie-Tooth disease (Zuchner et al. 2005). While Charcot–Marie-Tooth disease is clinically characterized by peripheral neuropathy, the relation between aging and *DNM2* gene expression remains undetermined. Disuse muscle atrophy related to decreased daily activity is commonly found in the elderly, but it is unclear whether exercise is effective for the maintenance of cognitive function.

Kelly et al. (2005) showed that β amyloid induces depletion of the DNM1 as well as DNM2 protein in cultured hippocampal neurons and the hippocampus of a Tg2576 mouse model of AD. On the other hand, dominant-negative DNM1, which selectively inhibits receptor-mediated endocytosis, raises the levels of mature amyloid precursor protein (APP) at the cell-surface, which is consistent with retention of APP on the plasma membrane, and endogenous Aβ secretion was significantly increased (Chyung and Selkoe 2003). It has also been shown that the location of β amyloid can be changed by decreased activity

of the DNM1 protein and that endocytosis affects the precision of PS-dependent epsilon-cleavage in cell culture (Fukumori et al. 2006). Whereas the DNM1 protein is specific for presynaptic terminals in the central nervous system (CNS), the DNM2 protein is ubiquitously expressed and, to our knowledge, does not exist in presynaptic terminals in the CNS. However, DNM2 has a similar structure to DNM1 and might also affect the sequestration and scavenging of β amyloid in relation to its axonal transport in peripheral nervous system.

We found that the expression of hippocampal *DNM2* mRNA was lower in the patients than in the control subjects, but this result should be carefully interpreted. We examined a small number of hippocampal tissue samples and used *β-actin* cDNA as an internal control; however, quantitative PCR revealed that the *β-actin* transcript is differently expressed in brain specimens of AD and control subjects (Gutala and Reddy 2004). Therefore, this decrease should be examined in the other brain areas and also in a larger number of samples using another internal control cDNA, such as *GAPDH* (Gutala and Reddy 2004). Alternatively, *DNM2* gene expression could be depleted in AD due to the widespread devastation of neurons, particularly in the hippocampus, as well as by β amyloid. Therefore, it remains to be determined whether the decrease in *DNM2* expression is the cause or the outcome of AD.

Acknowledgments We thank Drs. Y. Ikejiri, T. Nishikawa, H. Yoneda, Y. Moto, A. Sawa, S. Fujinaga, T. Matsubayashi, K. Taniguchi, Y. Ikemura and T. Mori for clinical evaluations, and E. Miyamura for assistance. This work was funded by the Future Program and the Japan Society for the Promotion of Science (JSPS), and by a Grant-in-Aid for Scientific Research on Priority Areas "Applied Genomics" from the Ministry of Education, Culture, Sports, Science and Technology of Japan.

References

Barrett JC, Fry B, Maller J, Daly MJ (2005) Haploview: analysis and visualization of LD and haplotype maps. Bioinformatics 21:263–265

Blacker D, Bertram L, Saunders AJ, Moscarillo TJ, Albert MS, Wiener H, Perry RT, Collins JS, Harrell LE, Go RC, Mahoney A, Beaty T, Fallin MD, Avramopoulos D, Chase GA, Folstein MF, McInnis MG, Bassett SS, Doheny KJ, Pugh EW, Tanzi RE; NIMH Genetics Initiative Alzheimer's Disease Study Group (2003) Results of a high-resolution genome screen of 437 Alzheimer's disease families. Hum Mol Genet 12:23–32

Chyung JH, Selkoe DJ (2003) Inhibition of receptor-mediated endocytosis demonstrates generation of amyloid β-protein at the cell surface. J Biol Chem 278:51035–51043

Corder EH, Saunders AM, Strittmatter WJ, Schmechel DE, Gaskell PC, Small GW, Roses AD, Haines JL, Pericak-Vance MA (1993) Gene dose of apolipoprotein E type 4 allele and the risk of Alzheimer's disease in late onset families. Science 261:921–923

Farrer LA, Cupples LA, Haines JL, Hyman B, Kukull WA, Mayeux R, Myers RH, Pericak-Vance MA, Risch N, van Duijn CM (1997) Effects of age, sex, and ethnicity on the association between apolipoprotein E genotype and Alzheimer disease. A meta-analysis. APOE and Alzheimer disease meta analysis consortium. JAMA 278:1349–1356

Fukumori A, Okochi M, Tagami S, Jiang J, Itoh N, Nakayama T, Yanagida K, Ishizuka-Katsura Y, Morihara T, Kamino K, Tanaka T, Kudo T, Tanii H, Ikuta A, Haass C, Takeda M (2006) Presenilin-dependent gamma-secretase on plasma membrane and endosomes is functionally distinct. Biochemistry 45:4907–4914

Gabriel SB, Schaffner SF, Nguyen H, Moore JM, Roy J, Blumenstiel B, Higgins J, DeFelice M, Lochner A, Faggart M, Liu-Cordero SN, Rotimi C, Adeyemo A, Cooper R, Ward R, Lander ES, Daly MJ, Altshuler D (2002) The structure of haplotype blocks in the human genome. Science 296:2225–2229

Gutala RV, Reddy PH (2004) The use of real-time PCR analysis in a gene expression study of Alzheimer's disease post-mortem brains. J Neurosci Methods 132:101–107

Hedrick PW (1987) Gametic disequilibrium measures: proceed with caution. Genetics 117:331–341

Kang DE, Saitoh T, Chen X, Xia Y, Masliah E, Hansen LA, Thomas RG, Thal LJ, Katzman R (1997) Genetic association of the low-density lipoprotein receptor-related protein (LRP), an apolipoprotein E receptor, with late-onset Alzheimer's disease. Neurology 49:56–61

Kelly BL, Vassar R, Ferreira A (2005) β-amyloid-induced dynamin 1 depletion in hippocampal neurons. J Biol Chem 280:31746–31753

Kolsch H, Lutjohann D, Ludwig M, Schulte A, Ptok U, Jessen F, von Bergmann K, Rao ML, Maier W, Heun R (2002) Polymorphism in the cholesterol 24S-hydroxylase gene is associated with Alzheimer's disease. Mol Psychiatry 7:899–902

Kuwano R, Miyashita A, Arai H, Asada T, Imagawa M, Shoji M, Higuchi S, Urakami K, Kakita A, Takahashi H, Tsukie T, Toyabe S, Akazawa K, Kanazawa I, Ihara Y; The Japanese Genetic Study Consortium for Alzheimer's Disease (2006) Dynamin-binding protein gene on chromosome 10q is associated with late-onset Alzheimer's disease. Hum Mol Genet 15:2170–2182

McKhann G., Drachman D, Folstein M, Katzman R, Price D, Stadlan EM (1984) Clinical diagnosis of Alzheimer's disease; report of the NINCDS-ADRDA work group under the auspices of department of health and human services task force on Alzheimer's disease. Neurology 34:939–944

Nyholt DR (2004) A simple correction for multiple testing for SNPs in linkage disequilibrium with each other. Am J Hum Genet 74:765–769

Obar RA, Collins CA, Hammarback JA, Shpetner HS, Vallee RB (1990) Molecular cloning of the microtubule-associated mechanochemical enzyme dynamin reveals homology with a new family of GTP-binding proteins. Nature 347:256–261

Pericak-Vance MA, Bass MP, Yamaoka LH, Gaskell PC, Scott WK, Terwedow HA, Menold MM, Conneally PM, Small GW, Vance JM, Saunders AM, Roses AD, Haines JL (1997) Complete genomic screen in late-onset familial Alzheimer disease. Evidence for a new locus on chromosome 12. JAMA 278:1237–1241

Praefcke GJ, McMahon HT (2004) The dynamin superfamily: universal membrane tubulation and fission molecules? Nat Rev Mol Cell Biol 5:133–147

Sambrook J, Fritsch EF, Maniatis T (1989) Molecular cloning: a laboratory manual. 2nd edn. Cold Spring Harbor Laboratory Press, New York, pp 9.14–9.19

Selkoe DJ (2002) Alzheimer's disease is a synaptic failure. Science 298:789–791

Shpetner HS, Vallee RB (1989) Identification of dynamin, a novel mechanochemical enzyme that mediates interactions between microtubules. Cell 59:421–432

Strittmatter WJ, Weisgraber KH, Huang DY, Dong LM, Salvesen GS, Pericak-Vance M, Schmechel D, Saunders AM, Goldgaber D, Roses AD (1993) Binding of human apolipoprotein E to synthetic amyloid beta peptide: isoform-specific effects and implications for late-onset Alzheimer disease. Proc Natl Acad Sci USA 90:8098–8102

Suzuki DT, Grigliatti T, Williamson R (1971) Temperature-sensitive mutations in *Drosophila melanogaster*. VII. A mutation (para-ts) causing reversible adult paralysis. Proc Natl Acad Sci USA 68:890–893

Wenham PR, Price WH, Blandell G. (1991) Apolipoprotein E genotyping by one-stage PCR. Lancet 337:1158–1159

Wijsman EM, Daw EW, Yu CE, Payami H, Steinbart EJ, Nochlin D, Conlon EM, Bird TD, Schellenberg GD (2004) Evidence for a novel late-onset Alzheimer disease locus on chromosome 19p13.2. Am J Hum Genet 75:398–409

Yao PJ (2004) Synaptic frailty and clathrin-mediated synaptic vesicle trafficking in Alzheimer's disease. Trends Neurosci 27:24–29

Zuchner S, Noureddine M, Kennerson M, Verhoeven K, Claeyes K, De Jonghe P, Merory J, Oliveira SA, Speer MC, Stenger JE, Walizada G, Zhu D, Pericak-Vance MA, Nicholson G, Timmerman V, Vance JM (2005) Mutations in the pleckstrin homology domain of dynamin 2 cause dominant intermediate Charcot–Marie-Tooth disease. Nat Genet 37:289–294

MOLECULAR AND CELLULAR BIOLOGY, Jan. 2008, p. 165–176 Vol. 28, No. 1
0270-7306/08/$08.00+0 doi:10.1128/MCB.00863-07

Regulation of Notch Signaling by Dynamic Changes in the Precision of S3 Cleavage of Notch-1▽†

Shinji Tagami,[1]‡ Masayasu Okochi,[1]*‡ Kanta Yanagida,[1] Akiko Ikuta,[1] Akio Fukumori,[1] Naohiko Matsumoto,[1] Yoshiko Ishizuka-Katsura,[1] Taisuke Nakayama,[1] Naohiro Itoh,[1] Jingwei Jiang,[1] Kouhei Nishitomi,[1] Kouzin Kamino,[1] Takashi Morihara,[1] Ryota Hashimoto,[1] Toshihisa Tanaka,[1] Takashi Kudo,[1] Shigeru Chiba,[2] and Masatoshi Takeda[1]

Department of Post-Genomics and Diseases, Division of Psychiatry and Behavioral Proteomics, Osaka University Graduate School of Medicine, Osaka 565-0871, Japan,[1] and Department of Cell Therapy and Transplantation Medicine, University of Tokyo Hospital, Bunkyo-ku, Tokyo 113-8655, Japan[2]

Received 16 May 2007/Returned for modification 19 July 2007/Accepted 11 October 2007

Intramembrane proteolysis by presenilin-dependent γ-secretase produces the Notch intracellular cytoplasmic domain (NCID) and Alzheimer disease-associated amyloid-β. Here, we show that upon Notch signaling the intracellular domain of Notch-1 is cleaved into two distinct types of NICD species due to diversity in the site of S3 cleavage. Consistent with the N-end rule, the S3-V cleavage produces stable NICD with Val at the N terminus, whereas the S3-S/S3-L cleavage generates unstable NICD with Ser/Leu at the N terminus. Moreover, intracellular Notch signal transmission with unstable NICDs is much weaker than that with stable NICD. Importantly, the extent of endocytosis in target cells affects the relative production ratio of the two types of NICD, which changes in parallel with Notch signaling. Surprisingly, substantial amounts of unstable NICD species are generated from the Val→Gly and the Lys→Arg mutants, which have been reported to decrease S3 cleavage efficiency in cultured cells. Thus, we suggest that the existence of two distinct types of NICD points to a novel aspect of the intracellular signaling and that changes in the precision of S3 cleavage play an important role in the process of conversion from extracellular to intracellular Notch signaling.

Presenilin (PS)-dependent γ-secretase (PS/γ-secretase) mediates the degradation of transmembrane domains (TMs) in many type 1 receptors, including Notch and β-amyloid protein precursor (βAPP) (18, 52). Degradation of these receptors is characterized by sequential endoproteolysis: following shedding by cleavage in the extracellular juxtamembrane region, the receptors undergo PS-dependent intramembrane proteolysis, releasing amyloid-β (Aβ)-like peptides and intracellular cytoplasmic domains (ICDs) (5, 14). At least in the cases of βAPP, Notch, and CD44, cleavages of the C termini of Aβ-like peptides and of the N termini of ICDs in the TM are distinct. This process of cleavage at two sites is known as "dual cleavage" (33). The process of Aβ generation has been intensively studied, and it is suggested that Aβ is released by a series of sequential cleavages followed by the ICD generation (25, 36, 53). An unusual characteristic of this intramembrane proteolysis is that some of the cleavage sites can vary (42). The precision of cleavage can therefore be defined as the ratio of the cleavage at each site. For example, PS-dependent cleavage of βAPP at the γ site, which is associated with Alzheimer disease (AD), occurs mainly at residue 40 (γ40), producing Aβ40, and at residue 42 (γ42), producing Aβ42. A small increase in the proportion of γ42 to γ40 cleavage is consistently observed in many familial AD (FAD)-associated PS or βAPP mutants (42), but it is unclear whether such changes in the precision of PS-dependent intramembrane proteolysis have any biological effects.

Notch signaling, which is essential for development, is a type of local-cell signaling that participates in neurodegeneration and tumorigenesis (1). The canonical Notch pathway is mediated by the regulated intramembrane proteolysis pathway, in which Notch receptors undergo ligand-dependent sequential endoproteolysis via a series of enzymes, including PS/γ-secretase (8). The Notch-1 ICD (NICD), which is produced by PS/γ-secretase-mediated cleavage at site 3 (S3), translocates to the nucleus and participates in transactivation of target genes (40). Elimination of PS function results in the Notch phenotype, which includes disruption of segmentation during the development of many kinds of animals, demonstrating the importance of NICD generation (41).

The intensity of Notch signaling is crucial for cell fate decisions. For example, Notch haplo-insufficiency causes the "notched-wing" phenotype in *Drosophila* (9). Reduced Notch activity favors the γδ T-cell fate over the αβ T-cell fate, whereas a constitutively activated form of Notch produces a reciprocal phenotype (48). The endocytosis of Notch and its ligands plays a key role in the regulation of the signaling intensity (40), but the biochemical aspects regulating this process have not been well studied. N-terminal amino acid se-

* Corresponding author. Mailing address: Department of Post-Genomics and Diseases, Division of Psychiatry and Behavioral Proteomics, Osaka University Graduate School of Medicine, D3, Yamada-oka 2-2, Suita, Osaka 565-0871, Japan. Phone: 81-6-6879-3053. Fax: 81-6-6879-3059. E-mail: mokochi@psy.med.osaka-u.ac.jp.

† Supplemental material for this article may be found at http://mcb.asm.org/.

‡ These authors contributed equally to this work.

▽ Published ahead of print on 29 October 2007.

quencing revealed that S3 in mouse Notch-1 lies between Gly1743 and Val1744 (murine Notch-1 numbering) (39). Whether the site of S3 cleavage can vary has not been examined previously.

In this study, we found that there is diversity in the site of S3 cleavage, resulting in the production of two types of NICD with apparently distinct stability and ability to transmit Notch signaling in cultured cells. Our results suggest that the precision of PS/γ-secretase-mediated cleavage is important for determining the intensity of Notch signaling.

MATERIALS AND METHODS

Antibodies. To generate affinity-purified polyclonal N-terminal capping antibodies to NICD-S (anti-NT-S), rabbits were immunized with a synthetic peptide (SRKRR) corresponding to the N terminus of NICD-S(+3). We also prepared two kinds of affinity columns in which the N-terminal peptide of NICD-V (VLLSRKRR) or NICD-S (SRKRR) was conjugated to Sepharose 4B (Amersham). We isolated the fraction of the anti-NT-S antiserum that bound to the NICD-S(+3) column but not the NICD-V column (32). Anti-NT-L antiserum was raised against a synthetic peptide (LLSRKRR) corresponding to the N terminus of NICD-L(+1) and then purified by affinity chromatography on Sepharose 4B conjugated to the N-terminal peptide of NICD-L (LLSRKRR), followed by a second step of affinity chromatography on Sepharose 4B conjugated to the NICD-S peptide (SRKRR). Other antibodies were purchased from commercial sources as follows: anti-NT-V (V1744 antibody) from Cell Signaling; antinicastrin and antibody mN1A against Notch-1 from Sigma-Aldrich; antibody H114 against Jagged-1 and antitubulin from Santa Cruz Biotechnology; anti-early endosome antigen 1 and anti-GM130 from BD Transduction Laboratories; antibody 12CA5 against the HA epitope from Roche Diagnostics, Inc.; antibody 9E10 against the myc epitope from Zymed; and anti-Na-K ATPase from Upstate Biotechnology.

cDNA constructs. The cDNA encoding the mouse Notch-1 variant NEXT was previously described (33). NEXTΔC was generated by PCR-based mutagenesis using the QuikChange-II kit (Stratagene) with NEXT cDNA as a template. The mutant versions of NEXT and NEXTΔC were generated using the same kit. To generate expression constructs for polypeptides NICD-V, NICD-L (+1), and NICD-S (+3), cDNAs encoding Val, Leu(+1), and Ser(+3) as the N termini were subcloned into the pASK-IBA6 vector (IBA). *HES-1*-luc (a kind gift from Alain Israel) (16) and pGa981-6 (a kind gift from Georg W. Bornkamm) (21) were used as described. For more sensitive detection of *HES-1* promoter transactivation, we newly generated a *hairy and enhancer of split-Y* (*HES-Y*) construct containing four sequential RBP-Jκ binding sites in the *HES-1* promoter region.

Cell culture. We generated HEK293 cells expressing PS1 R278I (a kind gift from M. Nishimura) (27) or PS1 G384A (a kind gift from H. Steiner) (44). HEK293 cells expressing either wild-type (wt) or mutants of PS1 were previously described (31). These cells were transfected with wt, mutant NEXT, or mutant NEXTΔC. HeLa cells expressing Dyn-1 K44A (a kind gift from S. Schmid) were used as described and stably transfected with NEXT or NEXTΔC. CHO(r) cells (a gift from S. Shirahata) (29) were stably transfected with mouse Notch-1 or Jagged-1.

Cell-free Notch-1 cleavage assay. To obtain crude membrane fractions (CMFs), cells were homogenized in buffer (0.25 M sucrose and 10 mM HEPES, pH 7.4) containing a protease inhibitor cocktail (Roche), followed by centrifugation at 1,000 × *g* for 5 min. The postnuclear supernatant was further centrifuged at 100,000 × *g* for 30 min, and the resulting pellet was collected. This CMF was resuspended in 150 mM sodium citrate buffer (pH 6.4) containing a 4× concentration of protease inhibitor cocktail (Sigma-Aldrich) and 5 mM 1,10-phenanthroline (Sigma-Aldrich), incubated for 20 min at 37°C, and then centrifuged at 100,000 × *g* for 30 min (11).

Pulse-chase experiments. Pulse-chase experiments were performed as described previously (11, 30, 31, 33, 34).

Immunoprecipitation/MALDI-TOF MS. Immunoprecipitation and matrix-assisted laser desorption ionization–time-of-flight mass spectrometry (MALDI-TOF MS) analysis was carried out as described previously (11, 31, 33). The heights of the MS peaks and molecular weights were calibrated using angiotensin and bovine insulin β-chain as standards (Sigma-Aldrich).

Immunoprecipitation-immunoblotting and immunoprecipitation-autoradiography. Metabolically labeled or unlabeled lysates were lysed in radioimmunoprecipitation assay buffer (1% Triton X-100, 0.5% sodium deoxycholate, and 0.1% sodium dodecyl sulfate [SDS]) containing a protease inhibitor mix (Sigma-Aldrich). The cell lysates were centrifuged at 10,000 × *g* for 15 min, and the supernatant fractions were immunoprecipitated as indicated. Following 8% Tris-glycine (Tefco) or 10 to 20% Tris-Tricine (Invitrogen) SDS-polyacrylamide gel electrophoresis (SDS-PAGE), the gels were either transferred to a polyvinylidene difluoride membrane and probed with the indicated antibodies or dried and analyzed by autoradiography. To quantitatively measure the levels of NICD species in cultured cells, several doses of each NICD polypeptide were separated together with samples by SDS-PAGE and analyzed by immunoblotting with the corresponding N-terminal capping antibody. The chemiluminescence intensities were measured using an LAS3000 scanner, followed by analysis with Multi Gauge Ver3.0 software (Fuji Film). Biotinylated transferrin was semiquantitatively measured by chemiluminescence using the scanner, followed by analysis with the software.

Cell-cell association assay. For the detection of de novo NICD species, CHO(r) cells stably expressing Notch-1 were grown to confluence in 150-mm dishes (2×10^7 cells per dish) in triplicate. Next, 3×10^7 CHO(r) cells stably expressing Jagged-1 were spread over the Notch-1-expressing cells. After 8 h of coculture, the cells were collected. For the reporter assay, the procedure was the same, although it was carried out in a 12-well plate and the number of cells was reduced accordingly.

cDNA transfection and reporter assay. To examine the intensity of Notch signaling, we used a dual luciferase reporter assay system (Promega) as described by the manufacturer (31). Briefly, cells expressing Notch-1 or its derivatives in a 12-well plate were transiently transfected with 125 ng of *HES-Y* or pGa981-6 and 1.25 ng of the control *Renilla* luciferase reporter plasmid pRL-TK. The reporter assay was performed on the next day. Dyn-1 K44A expression was induced with various concentrations of tetracycline 24 h prior to transfection with *HES-Y*. Cell-cell association was performed 24 h after transfection with *HES-Y*.

Preparation of nuclear extract from mouse tissues. A nuclear complex co-IP kit (Active Motif) was used to obtain nuclear extracts from C57BL/6 (Japan SLC) mouse tissues. Homogenized adult mouse brain or fetal mouse tissues without internal organs (embryonic day 12) were treated according to the manufacturer's instructions. Subsequently, the nuclear extracts were diluted using the immunoprecipitation buffer included in the kit, precleared three times with protein G- or protein A-Sepharose, and immunoprecipitated according to the manufacturer's instructions.

Purification of polypeptides. NICD-V, NICD-L(+1), and NICD-S(+3) polypeptides fused with *strept*-tag-II followed by an N-terminal factor Xa cleavage site were obtained by transforming *Escherichia coli* (BL21) with pASK-IBA6 (IBA) encoding each polypeptide. Briefly, after the expression was induced, the cells were collected by centrifugation at 4,500 × *g* for 12 min, resuspended in ice-cold TSE buffer (10 mM Tris-HCl [pH 7.4], 20% sucrose, and 2.5 mM Na-EDTA), and then incubated on ice for 10 min. The cells were again collected by centrifugation, resuspended in ice-cold water, incubated for 10 min, briefly sonicated, and sedimented by centrifugation at 14,000 × *g* for 15 min (osmotic shock fractionation). The supernatant was passed through a Strep-Tactin Sepharose column (IBA). Bound polypeptides were eluted with phosphate-buffered saline containing 2.5 mM desthiobiotin. Eluted polypeptides were treated with factor Xa (Sigma-Aldrich), and the solution was passed through the column again to remove uncleaved polypeptide (34). The purity of the polypeptides was confirmed by 6% Tris-glycine SDS-PAGE, followed by staining with Coomassie brilliant blue.

Loading of polypeptides. The polypeptides obtained as described above were loaded into cells using Chariot protein transfection reagent (Active Motif) according to the manufacturer's instructions. Briefly, cells were grown and transfected with reporter genes in a 12-well plate. The cells were then loaded with 5 μg of each polypeptide or bovine serum albumin (BSA) along with 0.5 μg of β-galactosidase, using 15 μl of Chariot reagent per well. Finally, the cells were stained for β-galactosidase or used for the reporter assay.

In vitro degradation assay. NICD polypeptides (0.2 μg) were mixed with 60 μl of fresh rabbit reticulocyte lysate (Promega) and incubated at 37°C. Clasto-lactacystin (10 μM), MG262 (100 nM), and 4-hydroxy-5-iodo-3-nitrophenyl-acetyl-Leu-Leu-leucinal-vinyl sulfone (NLVS) (10 μM) were added to inhibit the action of the proteasome.

Transferrin uptake assay. To estimate the rate of endocytosis, the levels of internalized and surface-bound biotinylated-transferrin were measured as described previously (11).

Subcellular fractionation. Linear gradients of 2.5% to 25% iodixanol (Optiprep; Axis-Shield) were prepared, and fractionation was performed as previously described (11).

Statistical analysis. Experiments were performed at least three times unless otherwise indicated. Representative results are shown for cell-free immunoprecipitation/MALDI-TOF MS, immunoblotting, immunoprecipitation-autoradiog-